Supporting Information

Tang et al. 10.1073/pnas.1402074111

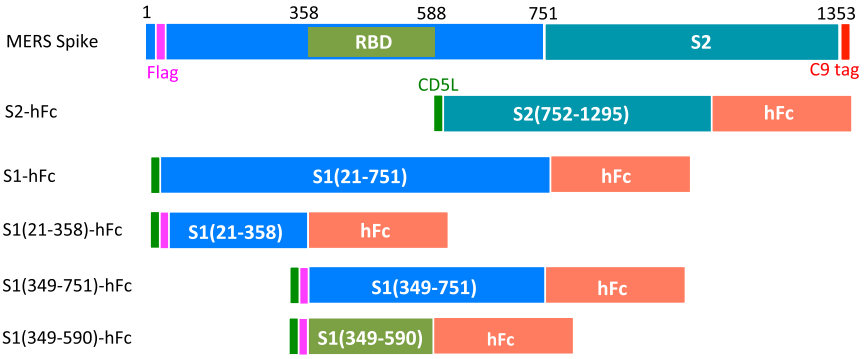

Fig. S1. Schematic representation of the Middle East Respiratory Syndrome coronavirus (MERS-CoV) Spike protein (S) and soluble S constructs used in this study. hFc, the hinge-CH2–CH3 of the human IgG1 heavy-chain constant region.

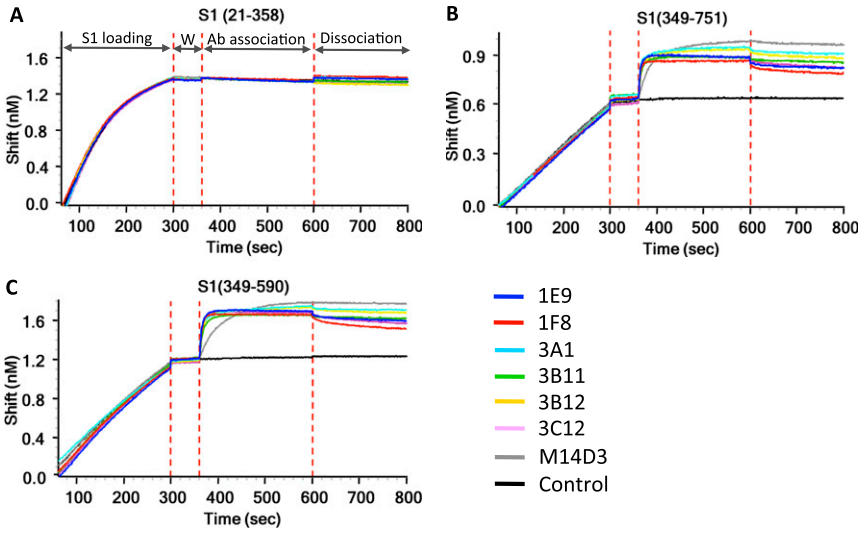

Fig. S2. Epitope mapping with three fragments of S1. Anti-Flag biosensors were immobilized with 10 μg/mL S1(21–358)-hFc (*A*), S1(349–751)-hFc (*B*), and S1(349–590)-hFc (*C*). After washing, each sensor was exposed to 100 nM of each single-chain variable domain fragment/crystallizable fragment (scFvFc). Additional shifting during the Ab loading step indicates its binding to the S1 fragment immobilized on the sensor. F10 was used as a nonbinding control.

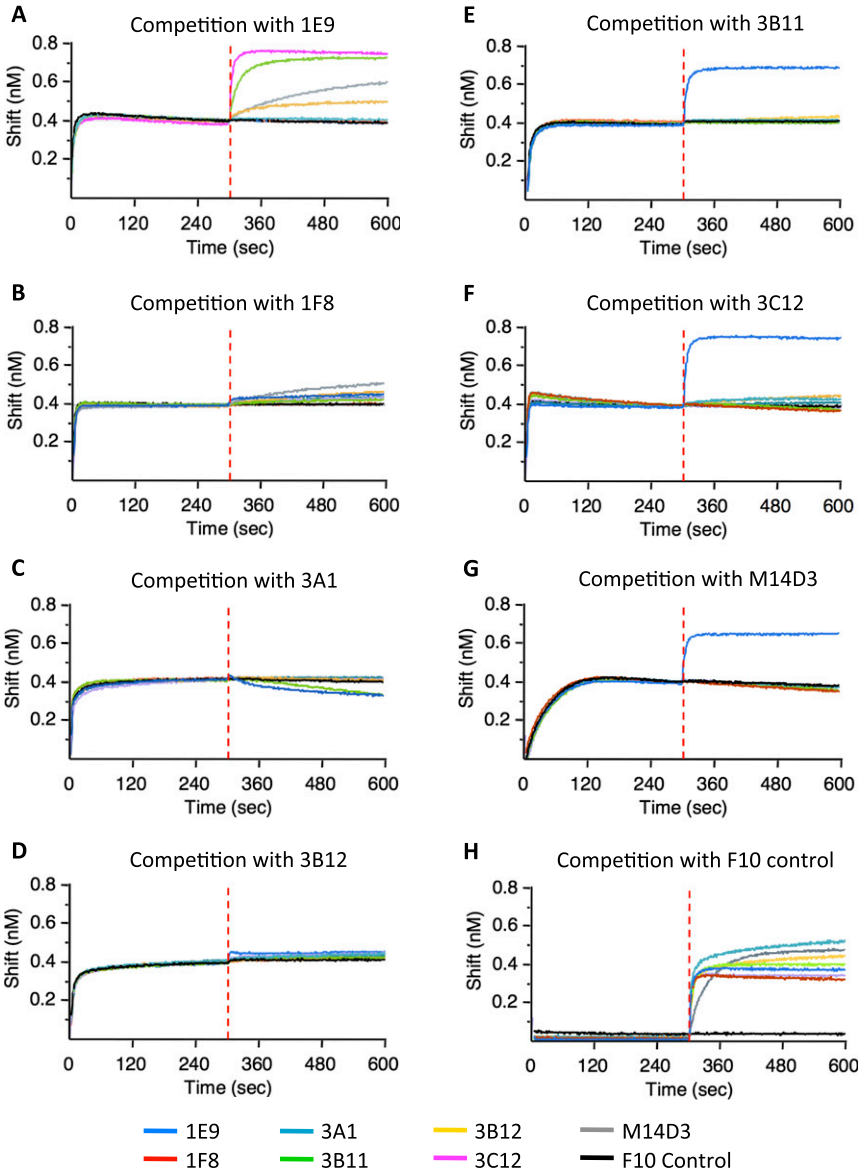

Fig. S3. Competition studies among different anti-S1 scFvFcs to S1 receptor-binding domain (RBD). Immobilized S1(349–590)-hFc first was saturated with 100 nM of 1E9 (*A*), 1F8 (*B*), 3A1 (*C*), 3B12 (*D*), 3B11 (*E*), 3C12 (*F*), or M14D3 (*G*) or with the F10 control (1), which recognizes the influenza A stem domain (*H*) (1). The capacity of an additional anti-S1 scFvFc binding to the sensors was monitored by measuring further shifts after injecting the second anti-S1 scFvFc (100 nM) in the presence of the first scFvFc (100 nM). The red dotted vertical line represents the second scFvFc loading time. F10 was used as a non-S1 binding control.

1. Sui J, et al. (2009) Structural and functional bases for broad-spectrum neutralization of avian and human influenza A viruses. *Nat Struct Mol Biol* 16(3):265–273.

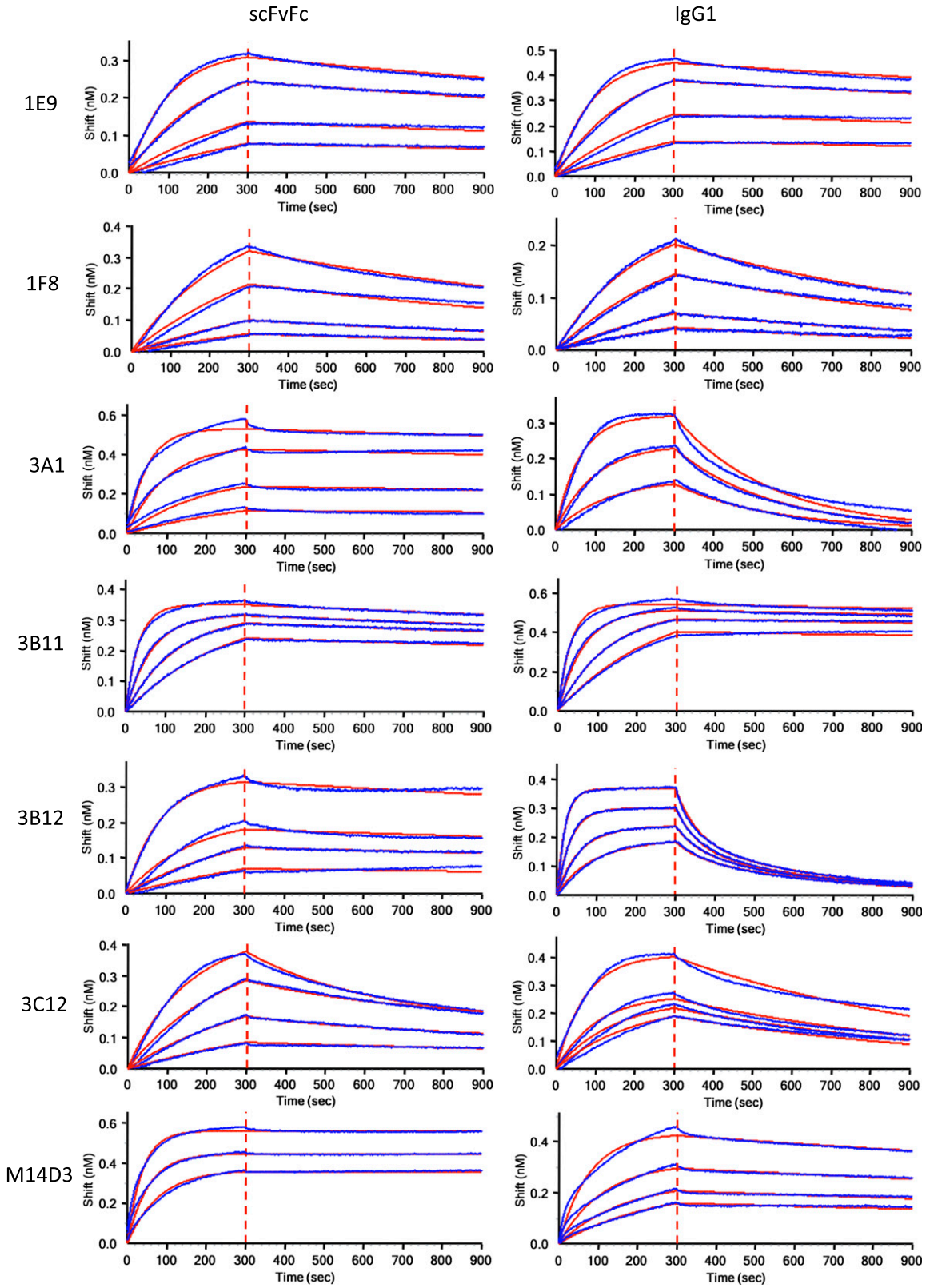

Fig. S4. Kinetic characterization of the binding of anti-S1 scFvFcs and IgGs to S1(349–590)-hFc. Purified S1(349–590)-hFc was immobilized onto anti-Flag biosensors, and various concentrations of each Ab were injected over the sensor surface. Binding kinetics were evaluated using a 1:1 binding model generated in Fortebio Data Analysis 7.0 software. Blue curves represent the experimental trace, and red curves represent the best global fits for the data used to calculate the K_d, K_{on}, and K_{off} (summarized in Table 1).

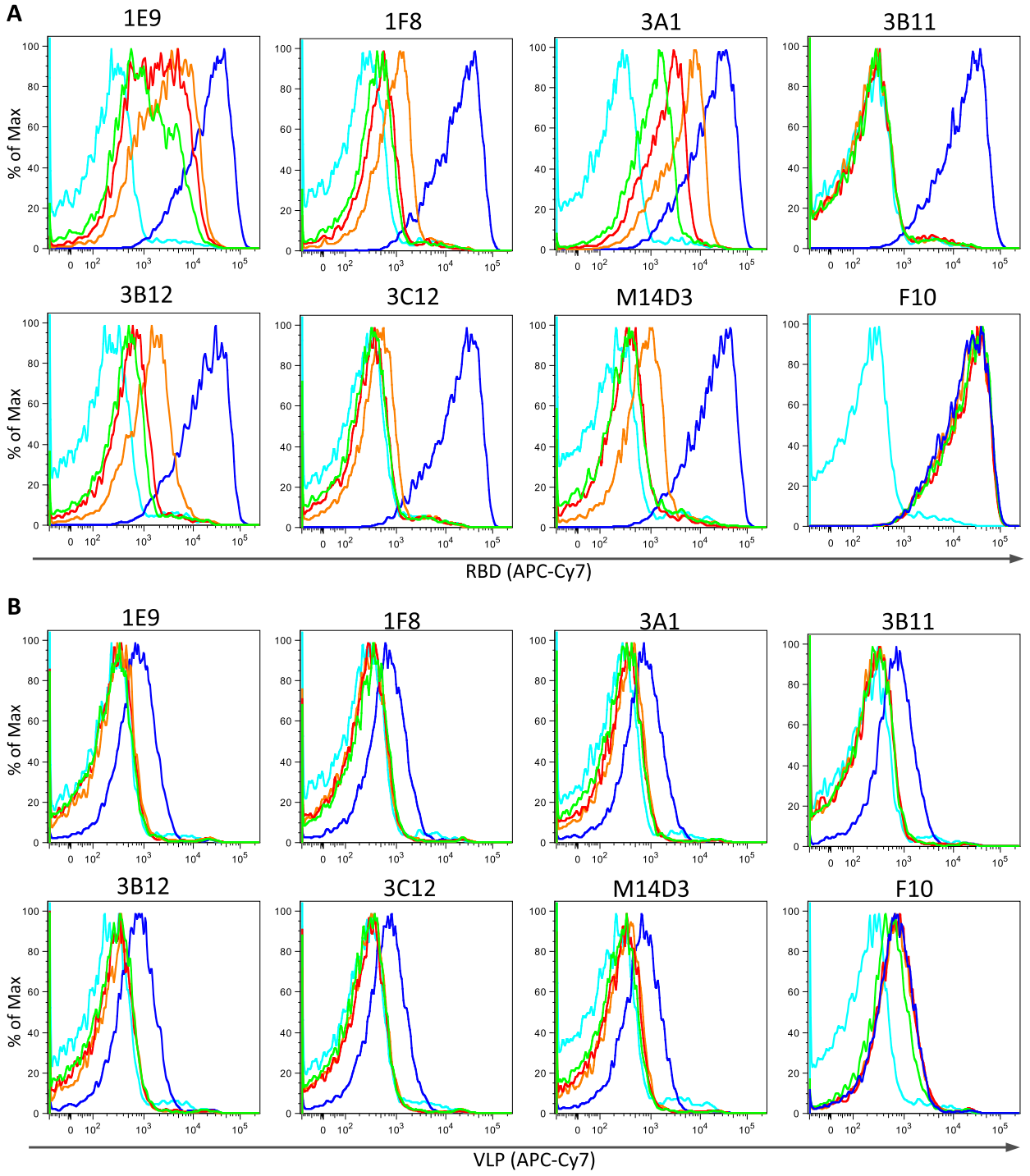

scFvFc (nM)	450	150	50	0	450
RBD (nM) or VLP (μl)	50	50	50	50	0

Fig. S5. Inhibition of MERS S1-RBD binding to hDPP4-expressing cells by anti-S1 scFvFcs. scFcFv Abs (0, 50, 150, or 450 nM) were used to block (*A*) 50 nM of soluble RBD-hFc or (*B*) 50 μL of MERS-S pseudotyped lentiviruses (VLP) binding to the 293T-hDPP4 cells. Binding was analyzed by flow cytometry. Each Ab is specified above its histogram. The color key for the Ab concentrations is given at the bottom of the figure.

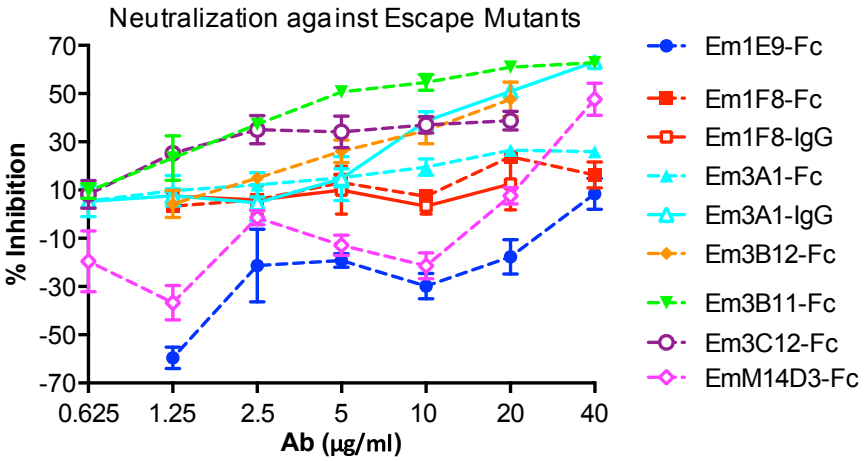

Fig. S6. The plaque reduction neutralization test ($PRNT_{50}$) assay for escape mutant viruses against their selecting Abs. Abs were diluted in PBS (2× serial dilutions, starting at 40 μg/mL) and were used to block infection with100 pfu of escape mutant MERS-CoV in Vero cells. Virus with no Abs was used as control. Plaques formed in each dilution were counted 48–72 h postinfection.

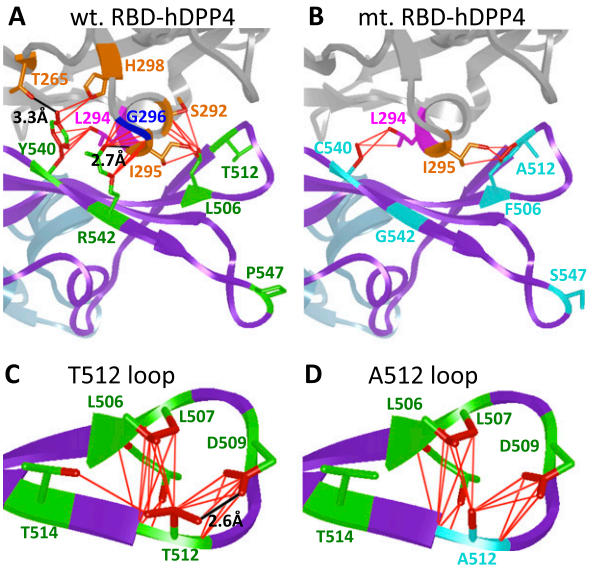

Fig. S7. Structural details of the interfaces between human dipeptidyl peptidase 4 (hDPP4) and MERS S wild-type or mutant RBDs. The interface structure was adapted from PDB ID code 4KR0, with hDPP4 displayed in gray and the Spike RBD represented as the receptor-binding motif in purple and the receptor-binding core in light blue. Five escape mutation residues are indicated in green before mutation (*A* and *C*) and in cyan after mutation (*B* and *D*). The hDPP4 residues 265, 292, 294–296, and 298 in contact with the mutations in RBD are labeled. The van der Waals (VDW) interactions are shown as red lines. Hydrogen bonds at S7A and S7C are shown as black lines.

Table S1. Abs' IC_{50} against wild-type and escape mutant virus

	Escape mutation		IC_{50}, μg/mL	
Selecting Ab	Nucleotide	Amino acid	Wild type	Mutation
1E9-Fc	C23089U	P547S	3.21	>40
1F8-Fc	A23074G	R542G	6.27	>40
1F8-IgG	G23076C, U25136C	R542S; I1229T	4.05	>40
3A1-Fc	G23075C/U	R542T	1.46	>40
3A1-IgG	G23075A	R542K	4.50	20
3B12-Fc	A22984G, C22966U	L506F, T512A	1.25	>20
M14D3-Fc	G23075A	R542K	4.30	>40
3B11-Fc	A23069G, C22966U	L506F, Y540C	1.83	6.76
3B11-IgG	NA	NA	3.50	NA
3C12-Fc	U23068C	Y540H	2.00	>40

NA, not available because no escape mutant was isolated from 3B11-IgG.

Table S2. K_d values of RBD mutants binding to the scFvFcs and hDPP4 (10^{-10} M)

RBD mutant	Selecting Ab	1E9	1F8	3A1	3B12	3B11	3C12	M14D3	hDPP4
L506F	3B11, 3B12	2.15 (0.52)	10.8 (0.68)	2.61 (1.16)	6.42 (3.65)	3.30 (2.44)	15.1 (0.75)	3.62 (7.7)	307 (1.43)
T512A	3B12	—	—	—	—	—	—	—	—
Y540C	3B11, 3C12	4.49 (1.09)	—	—	—	—	—	—	—
R542G	1F8, 3A1, M14D3	—	—	—	—	—	—	—	—
P547S	1E9	—	23.7 (1.5)	6.27 (2.79)	9.26 (5.26)	1.70 (1.26)	19.5 (0.97)	1.68 (3.57)	182 (0.85)
L506F, T512A	3B12	—	—	—	—	—	—	—	—
L506F, Y540C	3B11	3.80 (0.92)	—	—	—	—	—	—	—
Wild-type RBD		4.13	15.8	2.25	1.76	1.35	20.1	0.47	214

Numbers in parentheses are K_d ratios divided by K_d of Ab or hDPP4 binding to wild-type RBD. –, undetectable.

Table S3. IC_{50} for neutralization of selected neutralizing Ab escape mutant viruses (μg/mL)

Ab	Em1E9-Fc (group 1)	Em1F8-Fc (group 2)	Em3B11-Fc (group 3)	Em3C12-Fc (group 3)
1E9-Fc	>40	<0.625	0.84	<0.625
1F8-Fc	12.8	>40	11.2	>40
3B11-Fc	1.50	0.88	6.76	8.94
3C12-Fc	<0.625	11.7	13.8	>40

Table S4. Contact change between five key RBD residues and neighboring amino acids (distance ≤5.0 Å) before and after mutation

Wild-type RBD	VDW contact	Mutant RBD	VDW contact
With hDPP4			
L506	7	F506	3
T512	0	A512	0
Y540	7	C540	3
R542	11	G542	0
P547	0	S547	0
Within RBD			
T512	20	A512	15

Detailed contacts are shown in Fig. S7.